Statistical uncertainty of cyclic resistance of sand under constant volume direct simple shear

Yue Sun[1#], *Bruno* Stuyts[1], and *Wim* Haegeman[1]

[1]*Laboratory of Geotechnics, Civil Engineering Department, Ghent University*
Technologiepark 68 B-9052, Gent, Belgium
[#]*Corresponding author: yuesun.sun@ugent.be*

ABSTRACT

In the design work of offshore foundations, such as monopiles and gravity platforms, the cyclic resistance of soil plays a critical role in assessing the effect of cyclic loading induced by wind, waves, and rotor dynamics during the operational lifetime. However, the cyclic behaviour of soil is often derived from only a limited number of laboratory tests, which can lead to inaccurate estimates of soil behaviour. Furthermore, this imprecision can affect the parameters selection for the design process. To gain a better understanding of the limitations and uncertainties associated with laboratory experiments, a series of cyclic direct simple shear (cDSS) tests are conducted on marine sand. Four combinations of consolidation stress and void ratio are selected, and a constant volume cDSS test is repeated a substantial number of times for each combination. This dataset captures the measurement uncertainty on the cyclic soil resistance. By analysing the variability of the results, the statistical distributions for the cyclic soil resistance parameters can be determined (e.g. number of cycles to reach a certain shear strain level). The same specimen exhibits slightly different strain-stress relationships due to the inherent variability of sand. Statistical methods are used to describe the cyclic resistance of the sand.

Keywords: cyclic DSS; constant volume; uncertainty; sand.

1. Introduction

The dynamic loading on offshore constructions, induced by wind and waves, can be significant. The dynamic behaviour of soil in response to these cyclic loads plays a pivotal role in the design process (Andersen 2015). Dynamic loading can potentially reduce foundation resistance compared to static loading, which can primarily be attributed to the accumulation of pore pressure and the collapse of the soil microstructure. To assess the dynamic resistance of soil, dynamic triaxial tests, cyclic torsional simple shear, and cyclic direct simple shear (cDSS) tests are widely accepted methods in the laboratory (Tatsuoka et al. 1986). The dynamic triaxial test apparatus applies cyclic shear stress in a plane at an angle of 45 ° to the horizontal plane during undrained testing. In a hollow cylinder torsional shear test, the shear load can be applied along the horizontal plane. However, the specimen preparation procedure for the tests is often challenging. The cDSS test induces a pure shear condition on the soil along the horizontal plane (Ye, Lu, and Ye 2015; Ulmer et al. 2019; Nong, Park, and Lee 2021). It effectively simulates the stress conditions experienced at the tip of monopiles and the base of suction caissons.(Andersen and Lauritzsen 1988).

In design practice, the reduction of strength and stiffness of sand due to cyclic loading is typically addressed by reducing the strength and stiffness parameters in numerical simulation models. The extent of this reduction is often derived from empirical diagrams and limited laboratory experiments, making it challenging to precisely eliminate the uncertainty. Notably, for cDSS tests on a kind of sand under a given relative density and consolidated to a selected consolidation stress, the number of cycles required to reach a specific shear strain tends to exhibit fluctuations influenced by various factors. This intrinsic uncertainty, if not appropriately considered in the design process, can result in unexpected responses in foundation behaviour.

Various researchers performed investigations aimed at mitigating this uncertainty and enhancing the precision of the cDSS test. For instance, Konstadinou et al. (2021) discussed the impact of apparatus stiffness in constant volume cDSS tests. Their findings suggested that maintaining a low ratio of stiffness between the sand specimen and apparatus can effectively minimize the influence of equipment compliance. Similarly, Baxter et al. (2010) conducted a comparative analysis of two lateral confining methods, namely wire membrane and ring stacks. Notably, the rings were found to offer increased lateral stiffness during consolidation, but with more than 15% greater confining system resistance compared to wire membrane. Eseller-Bayat and Gulen (2020) conducted a series of tests to study the influence of preparation methods, including air pluviation, wet tamping, and moist under compaction. They found the optimum method for fully saturated specimens is moist tamping.

The examples mentioned above pay attention to the uncertainty of the test method. However, the inherent uncertainty in the cDSS test results still lacks adequate investigation, particularly in terms of statistical uncertainty. In this research, four combinations of consolidation stress and relative density are selected and then thirty tests are performed for each condition.

Statistical methods are adopted to assess the test procedure and results. Statistical distributions are fitted to selected test outputs.

2. Test Procedure

This study focuses on a clean fine to medium sand from the Belgian North Sea. To ensure its purity, large shell debris is removed by a sieve before sample preparation. The particle size distribution (PSD) obtained with the sieve method is shown in Figure 1. The median grain size (d_{50}) and uniformity coefficient (C_u) of the sand are computed at $d_{50} = 0.15$ mm, and $C_u = 1.2$, respectively. The specific gravity of the sand particle is found to be $G_s = 2.65$, which is determined through the particle density test. Additionally, the extreme void ratios are identified as $e_{max} = 0.77$ and $e_{min} = 0.56$, which are determined by ASTM methods.

A computer-controlled two-way cyclic direct simple shear apparatus, produced by Wille Geotechnik, is used for the experiment procedures. Cylindrical sand specimens with dimensions of 71.37 mm in diameter and 22.05 mm in height are prepared using dry pluviation. The lateral confining is achieved by a stack of rigid steel rings, with each ring having a thickness of 1mm. The DSS apparatus has a vertical Linear Variable Differential Transformer (LVDT) and a horizontal LVDT to monitor the specimen's deformation in two directions. In undrained conditions, a constant specimen volume is achieved by keeping the upper platform of the device in a fixed position. However, an alteration in vertical stress can result in minor vertical displacement, due to the elastic contract of device steel pillars, especially when the device stiffness is relatively low. To counteract the effects of device stiffness, an extension control model was employed to actively adjust the upper plane, guided by the feedback values from LVDT (Al Tarhouni and Hawlader 2021). The apparatus applies a sinusoidal shear stress over time during each shearing cycle, rather than abruptly applying or releasing maximum stress. The loading frequency, a critical factor influencing soil dynamic resistance, is set to 0.1Hz, which is representative of the wave loading frequency during extreme storms in the North Sea (Nikitas 2017).

The oven-dried sand is divided into three portions and funnelled into a membrane situated within the specimen mould. To achieve the desired height, the mould is subjected to vibrations induced by the impact of a hammer, thereby densifying the sand. In the meantime, the top surface of the sand specimen is levelled by a ruler. Subsequently, the sand specimen with the mould is relocated to the loading device and fixed. A 5kPa seating pressure is applied by the upper plate until contacting the specimen. Then, the mould is removed, and the specimen undergoes a consolidation process by a constant vertical stress. Given the research focus is offshore geotechnics, a pre-shear phase, comprised of 400 cycles of shear at 4% vertical stress, is designed to account for the stress history (Andersen 2015). During the pre-shear stage, the specimen is also allowed to consolidate under constant vertical stress. Before the initiation of the cyclic shearing phase, the control mode transitions from constant stress to constant volume. All tests are stopped when a one-side shear strain of 5% is reached.

In this study, four combinations of consolidation stress and relative density are selected. For each condition, a cDSS is test repeated 30 times. The name of each test combination is outlined in Table 1. The cyclic shear stress ratio (CSR), the ratio between cyclic shear stress and the reference vertical effective stress, is maintained at 10% for all groups. The cyclic shear stress values for two vertical stress conditions of 100kPa and 250kPa are calculated using the following equations.

$$\sigma'_{ref} = p_a \cdot (\sigma'_{vc}/p_a)^n$$

$$\tau_c = CSR \cdot \sigma'_{ref}$$

Where p_a is the atmospheric pressure and the n equals 0.9 for the cyclic shear strength of sand and silt. The empirical exponent n is determined to minimize the influence of consolidation stress (Andersen 2015).

Table 1. Test groups

Groups	Vertical Stress	Initial Dr
SL	100 kPa	40%
SD	100 kPa	80%
HL	250 kPa	40%
HD	250 kPa	80%

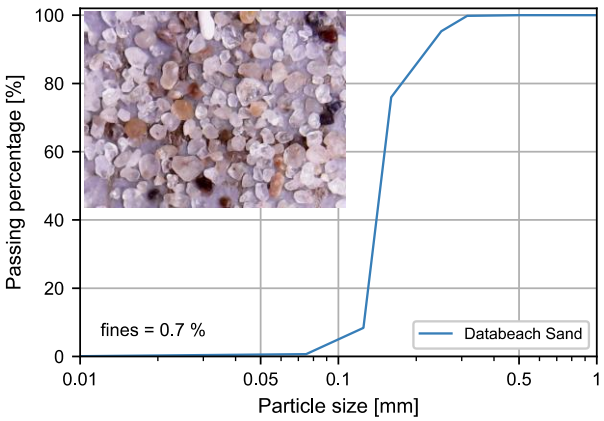

Figure 1. Particle size distribution and photo of the material.

3. Test Results and Discussion

3.1. Preparation quality

During consolidation, the specimens undergo unavoidable compression, resulting in a minor increase in relative density. A corrected relative density (D_r') is necessary to verify the quality and degree of uncertainty in the preparation procedures of the specimens prior to the shear stage. A good specimen preparation can help minimise this change. The corrected relative density of the specimens is calculated based on the real specimen height after consolidation, accounting for changes during the specimen mounting and consolidation phases. The corrected relative density is illustrated in Figure 2, and detailed statistical parameters are provided in Table 2. The average value of the corrected relative density demonstrates an increase ranging from 3.2% to 8.7%.

Notably, loose specimens exhibit a larger increase compared to dense specimens under the same consolidation stress.

Furthermore, it is expected that a higher consolidation stress will result in greater compression in the sand specimens. In terms of the standard deviation (Std), all four groups exhibit similar small values, indicating that the effect of sample preparation on relative density is limited.

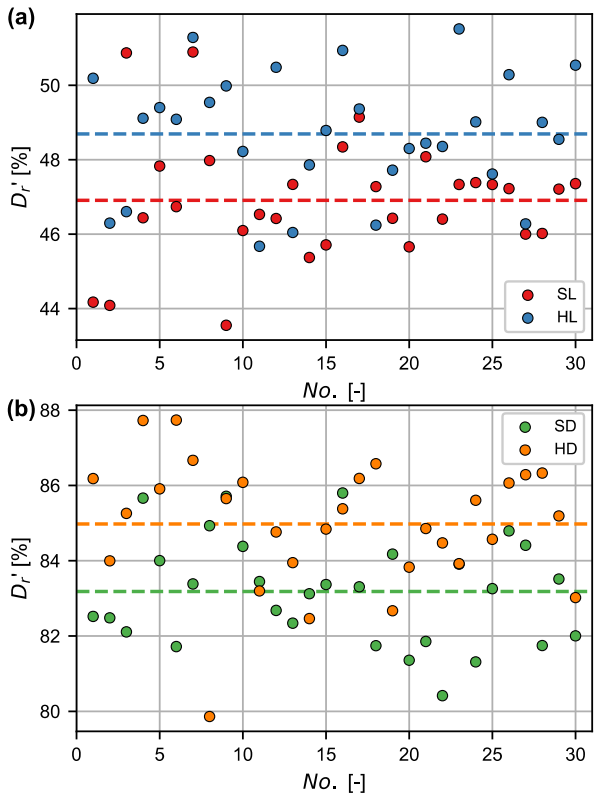

Figure 2. The corrected relative density D_r' of the specimens.

3.2. Stress-strain behaviour

Figure 3 illustrates the relationship between shear stress and shear strain for a single specimen from each group. At the onset of shearing, a nearly linear response in strain is observed, indicating an elastic deformation occurred with the shear stress rising and falling. However, with an increasing number of shear cycles, the strain-stress relationship transforms from a line into a hysteresis loop, and the shear strain does not revert to zero when the shear stress disappears. This phenomenon indicates the occurrence of plastic deformation, which amplifies with each cycle. The configuration of the hysteresis loop transitions from convex to concave when the strain is relatively large. Specimens with lower density (HL and SL) exhibit a more rapid collapse compared to dense specimens (HD and SD). For instance, the former merely requires two or three shear cycles to reach 5% strain, whereas the latter needs more than fifteen shear cycles. The strain expansion rate of the dense specimens is not uniform. When the plastic strain appears, and the strain is less than 2%, the expansion rate is higher than the rest of the part. As for the consolidation stress, the influence of V_s on the configuration of stress-strain behaviour is less than the influence of the density. This is evidenced by the fact that the HL and SL specimens exhibited similar shape patterns, as well as the HD and SD specimens.

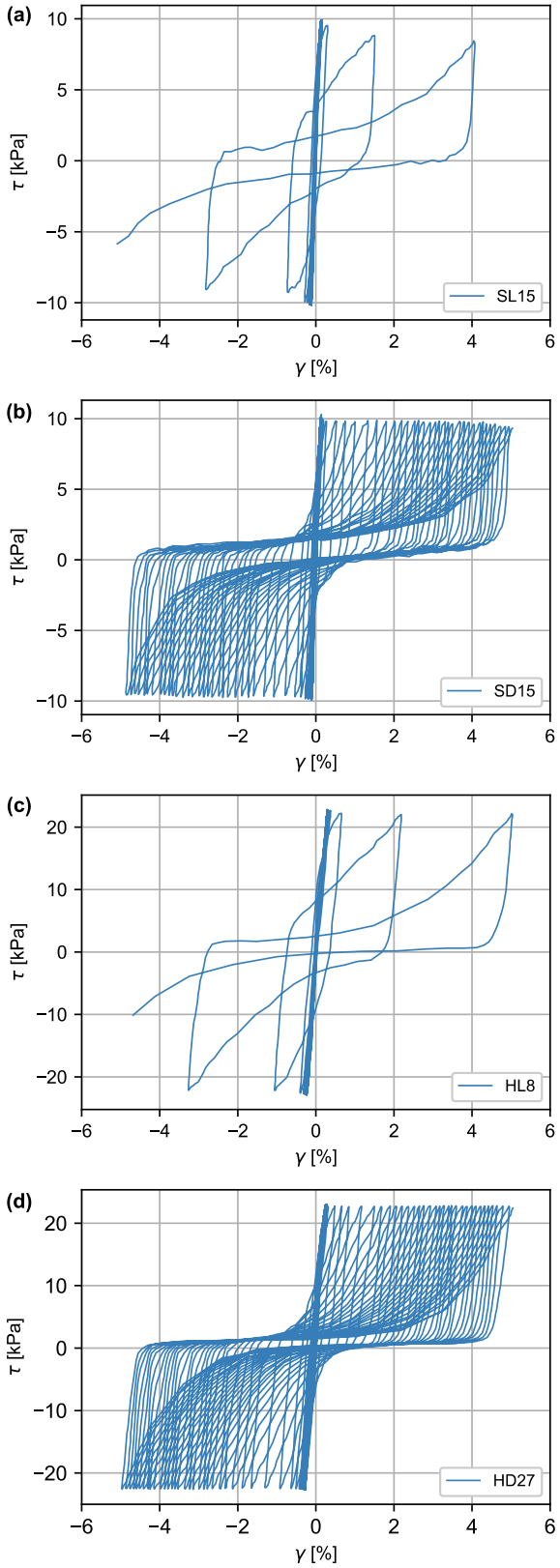

Figure 3. The stress-strain evolutions of the representative specimens.

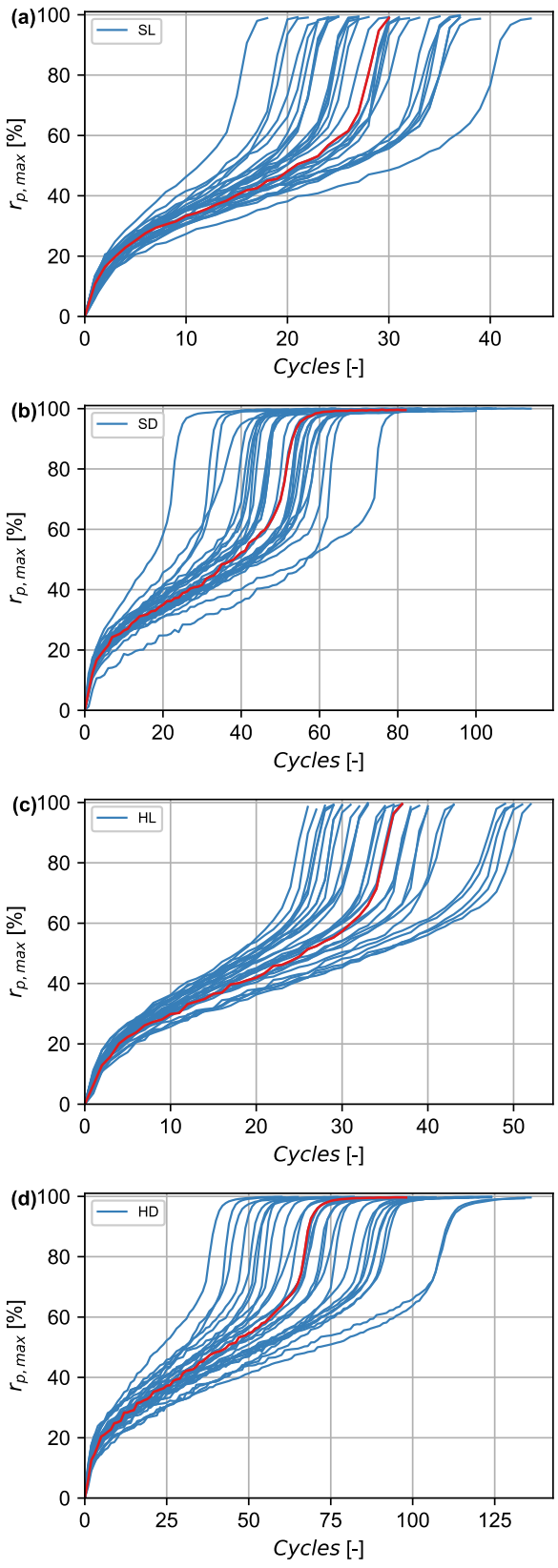

Figure 4. The variation of pore pressure ratios with the increasing of shear cycles.

Table 2. Statistical indexes for corrected relative density.

Groups	Mean	Std
SL	46.9%	1.6%
SD	83.2%	1.4%
HL	48.7%	1.6%
HD	85.0%	1.7%

3.3. Evolutions of pore pressure

The pore pressure, also referred to as excess pore pressure, is not directly measured by a sensor during shearing. Instead, it is postulated that the decrease in vertical stress is equivalent to the increase in pore pressure under constant volume conditions (Dyvik et al. 1987; Monkul et al. 2015; Ajmera, Brandon, and Tiwari 2019). The pore pressure mentioned in this paper is, therefore, an apparent pore pressure. The maximum pore pressure ratio ($r_{p,max}$) is defined as the ratio between the maximum pore pressure in a cycle and the initial vertical stress. In Figure 4, the pore pressure variations against the shear cycles for all specimens in the four groups are depicted, in which the red curves correspond to the specimens in Figure 3. The variation curves of $r_{p,max}$ rapidly increase at the onset of shear. Subsequently, the rate of the pore pressure ratio rising slows down when the value approaches approximately 0.35. After excessing 0.6, the ratio surges to 1, indicating the occurrence of liquefication. The specimens with low density reach the strain failure standard at the same time. However, the shear strain of the dense specimens has not yet reached the failure criterion. Then, the plastic strain of dense specimens increases with each cycle during liquefication.

The deviation of the number of shear cycles with the $r_{p,max}$ increasing is calculated to assess the variation in uncertainty for every group's $r_{p,max}$. The specific calculation method is as follows: initially, the number of shear cycles corresponding to the $r_{p,max}$ is calculated. Subsequently, the standard deviation of all shear cycle data at a certain $r_{p,max}$ within a group is computed. The pore pressure ratio curves originate at one point and accumulate deviation with the increasing cycles. The increasing trend of the standard deviation of cycles number ($N\ Std$) is shown in Figure 5. Most scatter occurs in the range between 20% and 60%, and the increase of standard deviation is basically linear. This suggests that uncertainty quantification should take the pore pressure stage into account.

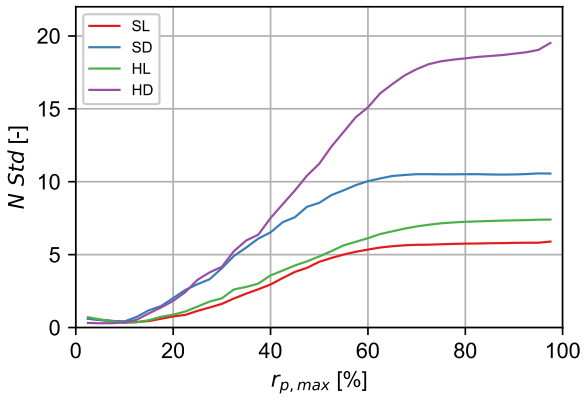

Figure 5. The variation of Std of N_f with the increasing of maximum pore pressure ratio.

Table 3. The statistical indexes of cycles at failure.

Groups	Min	Max	Mean
SL	18	44	29
SD	51	114	80
HL	26	52	37
HD	60	136	96
Groups	**Median**	**Std**	**CV**
SL	29	6.0	20%
SD	81	15.2	19%
HL	37	7.6	20%
HD	97	20	21%

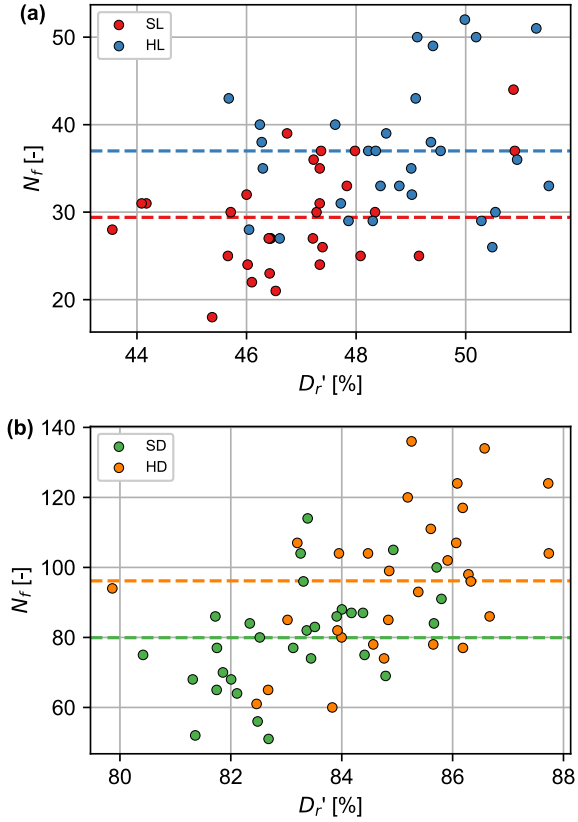

Figure 6. The distribution of N_f and Dr' of specimen.

3.4. Cycles number at failure strain

When the shear strain exceeds the failure strain criterion (5% one-side strain), the number of cycles at failure (N_f) is recorded. The test results of the cyclic number are presented against the axis of corrected relative density in Figure 6, in which the average values are presented by dotted lines. Under the same density condition, specimens subjected to high vertical stress exhibit increased resistance to shear cycles, irrespective of whether they are dense or loose. To analyse these discrete data points, statistical indices are calculated and tabulated in Table 3. The data points exhibit a broad range, with the maximum N_f nearly double the minimum N_f. The proximity of the mean and median values suggests a likely symmetrical distribution of N_f. Specimens with larger mean values of N_f typically exhibits a larger Std. It is widely acknowledged that relative density significantly influences the cycles at failure. To account for this factor, the coefficient of variation (CV) is introduced to compare the variability of the test results between different groups.

$$CV = \frac{Std}{Mean} \times 100\%$$

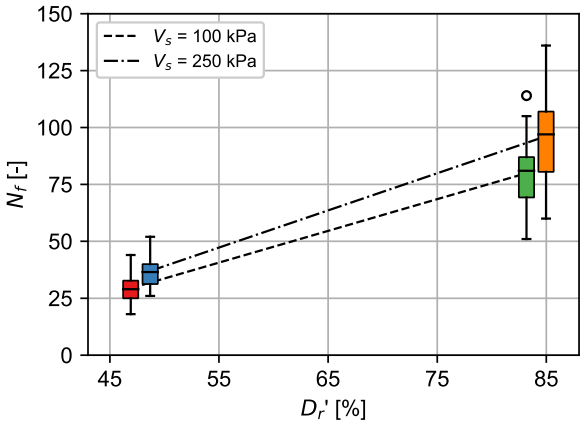

Figure 7. The deviation box of test results.

The CV for all groups is approximately 20%, suggesting that the uncertainty of N_f for this material can be described by this ratio, which is not affected by the specimen density. The box plot of four groups is depicted in Figure 7, which summarizes the data distribution and variance across different groups. The height of the box, equal to the interquartile range, exhibits an increasing trend with the rise of D_r'. This pattern indicates that the N_f values of the denser groups span a broader range and exhibit greater variation. The median values within the same V_s groups are interconnected by a line. It is noteworthy that the groups with higher V_s values are plotted above the line with smaller V_s. This arrangement implies that a value of 0.9 may have been overestimated to mitigate the impact of consolidation stress.

3.5. Distribution of test results

The N_f data exhibits a symmetric distribution, which satisfies the precondition for a Gaussian distribution. To evaluate whether N_f distributions conformed to a Gaussian distribution, a Shapiro-Wilk Test is used. This method is primarily used to estimate whether a small sample dataset ($n < 50$) follows a Gaussian distribution (Shapiro and Wilk 1965). In this research, the SL, SD, and HD groups demonstrate a high probability of conforming to a Gaussian distribution. However, the statistical significance of the HL group is lower than 0.05, indicating that it does not conform to a Gaussian distribution because it is influenced by three specimens that gather at the maximum boundary. In summary, the results of the cyclic DSS test have a high probability of fitting a Gaussian distribution, as described by the following probability equation.

$$f(N_f) = \frac{1}{\sigma_{N_f}\sqrt{2\pi}} exp(\frac{-(N_f - \mu_{N_f})^2}{2{\sigma_{N_f}}^2})$$

The above conclusion that the Std is approximately 20% of the mean value for every group combined.

$$\sigma_{N_f} = 0.2\mu_{N_f}$$

Subsequently, the result points can be normalized using the following equation.

$$N_f{}' = (N_f - \mu_{N_f})/\sigma_{N_f}$$

A comparison between the histogram of the test results and the standard Gaussian distribution curve is plotted in Figure 8. In this figure, the height of the bar closely aligns with the red line, demonstrating that the cyclic DSS test under undrained conditions for the sand can be reasonably assumed to follow a Gaussian distribution. Notably, this distribution has a standard deviation (Std) of 20% of the average value. Given these findings, it is worthwhile to incorporate this assessment of uncertainty from the laboratory test when designing a foundation subjected to cyclic loading.

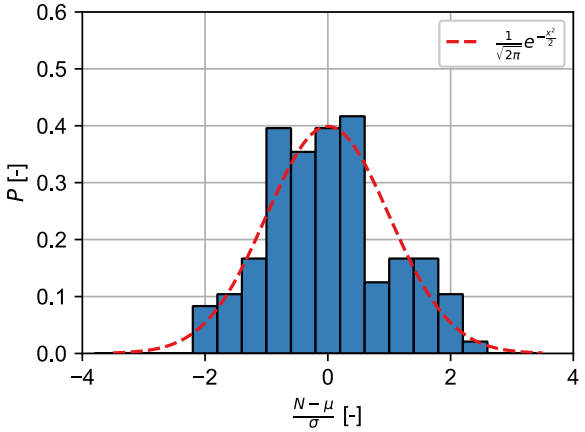

Figure 8. The probability distribution of normalized test results.

4. Conclusions

A cyclic direct simple shear test on sand is conducted 30 times under four selected conditions of consolidation pressure and relative density. The test results reveal the following conclusions:

Specimens transition from nearly elastic strain response during the initial shear to more and more plastic strain development with continued cyclic shear. Under the same consolidation stress, loose specimens exhibit rapid strain increases, while dense specimens experience a slower rise in strain.

The pore pressure ratio curves, originating from a single point, exhibit an accumulated deviation with each increasing cycle. Notably, pore pressure mainly scatters within the 20% to 60% range of $r_{p,max}$.

Both higher consolidation stress and higher density contribute to the specimens resisting more shear cycles, indicated by a higher mean N_f. Furthermore, the standard deviation increases in correlation with the number of cycles. The ratio between the standard deviation and the average of the failure cycle number remains constant across all four groups, at approximately 20%.

The distribution of the number of cycles to reach 5% strain was examined, revealing a high probability that the test results conform to a Gaussian distribution. The parameter Std can be assumed to be equal to 20% of the average. This finding can be valuable when accounting for the uncertainty of cyclic DSS for sand under undrained conditions.

Acknowledgements

The first author is grateful for the financial support provided by the China Scholarship Council. The authors would also like to acknowledge the support of the Belgian Ministry of Economic Affairs through the ETF project WINDSOIL project. The support of VLAIO through the De Blauwe Cluster SBO SOILTWIN project is also acknowledged.

References

Ajmera, B., Brandon, T. and Tiwari, B. 'Characterization of the Reduction in Undrained Shear Strength in Fine-Grained Soils Due to Cyclic Loading'. *J. Geotech. Geoenvironmental Eng.*, 145 (5), pp.04019017, 2019. https://doi.org/10.1061/(ASCE)GT.1943-5606.0002041.

Al Tarhouni, MA. and Hawlader, B. 'Monotonic and Cyclic Behaviour of Sand in Direct Simple Shear Test Conditions Considering Low Stresses'. *Soil Dyn. Earthq. Eng.*, 150 (November), pp.106931, 2021. https://doi.org/10.1016/j.soildyn.2021.106931.

Andersen, KH. 'Cyclic Soil Parameters for Offshore Foundation Design'. *Front. Offshore Geotech. III*, 5 2015.

Andersen, KH. and Lauritzsen, R. 'Bearing Capacity for Foundations with Cyclic Loads'. *J. Geotech. Eng.*, 114 (5), pp.540–55, 1988. https://doi.org/10.1061/(ASCE)0733-9410(1988)114:5(540.

Baxter, CDP., Bradshaw, AS., Ochoa-Lavergne, M. and Hankour, R. 'DSS Test Results Using Wire-Reinforced Membranes and Stacked Rings'. In *GeoFlorida 2010*, pp.600–607. Orlando, Florida, United States: American Society of Civil Engineers, 2010. https://doi.org/10.1061/41095(365)57.

Dyvik, R., Berre, T., Lacasse, S. and Raadim, B. 'Comparison of Truly Undrained and Constant Volume Direct Simple Shear Tests'. *Geotechnique*, 37 (1), pp.3–10, 1987. https://doi.org/10.1680/geot.1987.37.1.3.

Eseller-Bayat, EE. and Gulen, DB. 'Undrained Dynamic Response of Partially Saturated Sands Tested in a DSS-C Device'. *J. Geotech. Geoenvironmental Eng.*, 146 (11), pp.04020118, 2020. https://doi.org/10.1061/(ASCE)GT.1943-5606.0002361.

Konstadinou, M., Bezuijen, A., Greeuw, G., Zwanenburg, C., Van Essen, HM. and Voogt, L. 'The Influence of Apparatus Stiffness on the Results of Cyclic Direct Simple Shear Tests on Dense Sand'. *Geotech. Test. J.*, 44 (5), pp.20190471, 2021. https://doi.org/10.1520/GTJ20190471.

Monkul, MM., Gültekin, C., Gülver, M., Akın, Ö. and Eseller-Bayat, E. 'Estimation of Liquefaction Potential from Dry and Saturated Sandy Soils under Drained Constant Volume Cyclic Simple Shear Loading'. *Soil Dyn. Earthq. Eng.*, 75 (August), pp.27–36, 2015. https://doi.org/10.1016/j.soildyn.2015.03.019.

Nikitas, G. 'Predicting Long Term Performance of Offshore Wind Turbines Using Cyclic Simple Shear Apparatus'. *Soil Dyn. Earthq. Eng.*, 2017. https://doi.org/10.1016/j.soildyn.2016.09.010.

Nong, Z-Z., Park, S-S. and Lee, D-E. 'Comparison of Sand Liquefaction in Cyclic Triaxial and Simple Shear Tests'. *Soils Found.*, 61 (4), pp.1071–85, 2021. https://doi.org/10.1016/j.sandf.2021.05.002.

Shapiro, SS. and Wilk, MB. 'An Analysis of Variance Test for Normality (Complete Samples)'. *Biometrika*, 52 (3/4), pp.591–611, 1965. https://doi.org/10.2307/2333709.

Tatsuoka, F., Ochi, K., Fujii, S. and Okamoto, M. 'Cyclic Undrained Triaxial and Torsional Shear Strength of Sands for Different Sample Preparation Methods'. *Soils Found.*, 26 (3), pp.23–41, 1986. https://doi.org/10.3208/sandf1972.26.3_23.

Ulmer, KJ., Green, RA., Rodriguez-Marek, A. and Baxter, CDP. 'Quality Assurance for Cyclic Direct Simple Shear Tests for Evaluating Liquefaction Triggering Characteristics of Cohesionless Soils'. *Proc. XVII Eur. Conf. Soil Mech. Geotech. Eng.*, no. Geotechnical Engineering, foundation of the future pp.2511–18, 2019. https://doi.org/10.32075/17ECSMGE-2019-0470.

Ye, B., Lu, J. and Ye, G. 'Pre-Shear Effect on Liquefaction Resistance of a Fujian Sand'. *Soil Dyn. Earthq. Eng.*, 77 (October), pp.15–23, 2015. https://doi.org/10.1016/j.soildyn.2015.04.018.

D18 Committee. 'Test Method for Consolidated Undrained Direct Simple Shear Testing of Cohesive Soils'. ASTM International, n.d. Accessed 9 February 2023. https://doi.org/10.1520/D6528-17.